

# Surface-plasmon-assisted nanoscale photolithography by polarized light

D. B. Shao and S. C. Chen<sup>a)</sup>

*Department of Mechanical Engineering, The University of Texas at Austin, Austin, Texas 78712*

(Received 7 March 2005; accepted 19 May 2005; published online 16 June 2005)

We demonstrate that photolithography can be extended to a subwavelength resolution for patterning of virtually any substrate by exciting surface plasmons on both a metallic mask and a substrate. Without any additional equipment or added complexity to mask design, one-to-one pattern transfer has been achieved. In this letter, a polarized laser beam of 355 nm wavelength was used as light source to photoinitiate an 80 nm thick photoresist on a silicon substrate coated with titanium of 80 nm thick. Array of line apertures of 100 nm in width were made on gold film or titanium film deposited on a quartz substrate, serving as the mask. Simulation results by finite-difference time-domain method have shown that surface plasmons excited on both the metallic mask and the Ti shield help to spatially confine the light behind the apertures. Experimental results show a strong dependence of pattern transfer on the polarization of light as well as the energy dosage of the light. The feature size using such method could be further scaled down, limited theoretically by the validity of the dielectric function of the material, and practically by the fabrication of the mask.

© 2005 American Institute of Physics. [DOI: 10.1063/1.1951052]

Photolithography has been a key technique in microfabrication over the past several decades because of its high throughput, low cost, simplicity, and reproducibility. However, the resolution is limited at the submicron scale by optical diffraction.<sup>1</sup> Enormous research efforts have been devoted to developing subwavelength lithography techniques, which, unfortunately, are complex and expensive. Among the many different lithographic approaches that can overcome the diffraction limit, such as electron-beam lithography (EBL), imprint lithography, and scanning probe lithography, near-field optical lithography<sup>2-4</sup> most closely resembles traditional photolithography, although limited by low transmission, low contrast, and low density.

The recent discovery of extraordinary transmission through a perforated metal films<sup>5-7</sup> has offered new possibilities in the realm of nanolithography, coined surface-plasmon-assisted lithography,<sup>8,9</sup> however arbitrary pattern transfer has still not been achieved. This approach stems from the strong surface electromagnetic (EM) mode characteristic of metals, which can couple to external transverse radiation, dramatically enhancing the transmission of light through subwavelength apertures in a mask.<sup>10</sup> The transmissivity appears to be a function of periodicity, aperture size, as well as wavelength.<sup>5</sup> The transverse electric (TE) and transverse magnetic (TM) modes have different cut-off frequencies when the aperture width is small.<sup>11</sup>

In this letter, the surface plasmons excited on the mask enhance the light through the subwavelength aperture, while the surface plasmons excited on the substrate help to confine the light intensity to the space behind the mask aperture by coupling to the light. The schematic representation of the setup is shown in Fig. 1(a). A polarized laser beam of 355 nm wavelength was used as the light source to expose an 80 nm thick photoresist on an 80 nm Ti film on a silicon substrate. The nanolithography mask was fabricated by first patterning lines of 950 K poly(methylmethacrylate) on a quartz

substrate using EBL. The linewidth was 100 nm with a periodicity of 1  $\mu\text{m}$  or 500 nm. Because of the small linewidth as well as the high density of the pattern, the electron-beam dosage was modulated and a developer of 40:1 isopropyl alcohol and methyl isobutyl ketone was employed for EBL. The mask [Figs. 1(b) and 1(c)] was then obtained by depositing 70 nm gold or titanium using electron-beam evaporation and lift off. Each mask pattern consists of two sets of line apertures perpendicular to one another. During our experiments, the polarization of the laser light was always kept in such a direction that one set of lines was parallel to the light polarization, while the other perpendicular. SU-8 (Microchem<sup>®</sup>), a negative near-UV photoresist (refractive in-

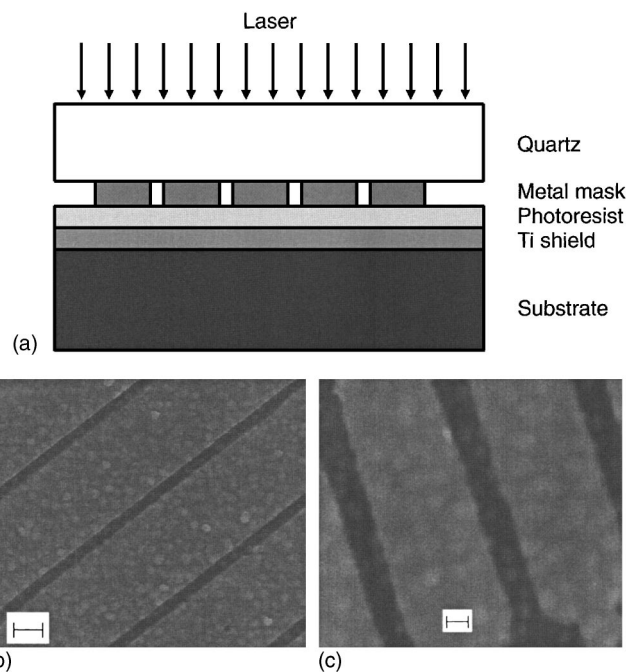


FIG. 1. A schematic view of the experimental setup (a) and scanning electron microscopy pictures of metallic mask patterns with (b) 1  $\mu\text{m}$  periodicity (scale bar 300 nm), and (c) 500 nm periodicity (scale bar 100 nm).

<sup>a)</sup> Author to whom correspondence should be addressed; electronic mail: scchen@mail.utexas.edu

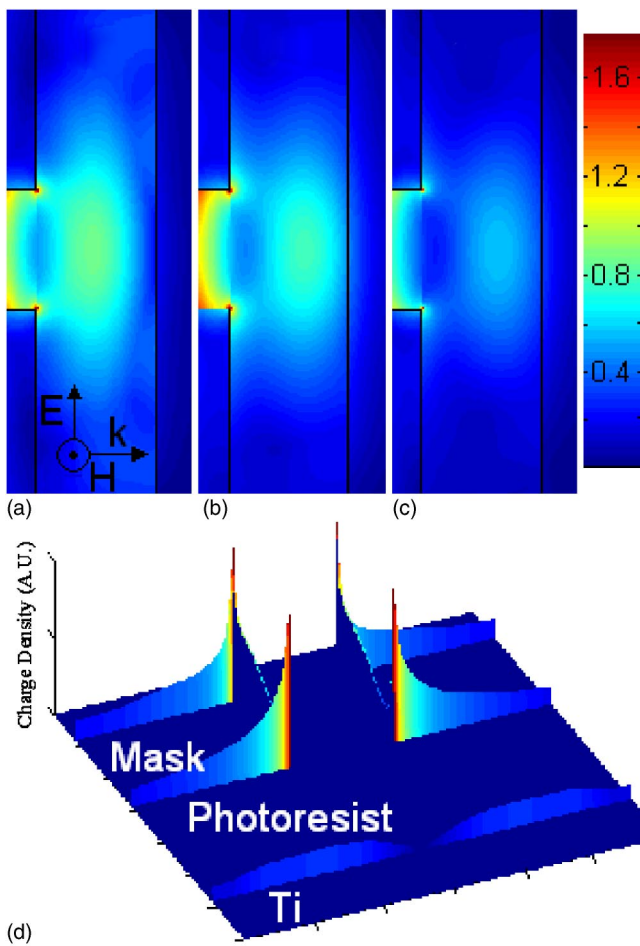


FIG. 2. (Color online) FDTD simulation results of electric-field distribution in the photoresist with: (a) A gold mask and bare silicon substrate, (b) a gold mask and Ti shield on Si substrate, (c) a Ti mask and Ti shield on Si substrate, (d) FDTD simulation results of maximum absolute values of charge density distribution with a Ti mask and Ti shield. The illustration of EM fields is TM mode. The charge densities on the two sides of centerline have opposite signs.

dex  $\sim 1.67$ ) was spun on the Ti-coated silicon substrate to a thickness of 80 nm.

Photoresist has a threshold illumination energy density. Only above this threshold can it be photoinitiated. To calculate the field distribution in the photoresist for different configurations, we have developed a two-dimensional TM mode finite difference time domain (FDTD) code. The FDTD method solves EM problems by elegantly discretizing the differential form of Maxwell's equations. Traditional FDTD method has stability problems when dealing with metals at optical frequencies due to negative dielectric constant. In our model, the refractive indices and extinction coefficients of the metals were first determined<sup>12</sup> and fitted with the Drude model, and then incorporated to the FDTD code.<sup>13</sup> To verify the accuracy of the program, the FDTD code was benchmarked with two-dimensional theoretical solutions of the scattering of light by a cylinder.<sup>14</sup> By integrating the current flowing in and out of each cell, one can calculate the charge density distribution. The results of the electric-field amplitude distribution between the mask and substrate through an aperture are plotted in Fig. 2. For a bare silicon substrate [Fig. 2(a)], not only does the light spread in the lateral direction, but its intensity at the interface between the photoresist and substrate is weakened. This explains why photolithogra-

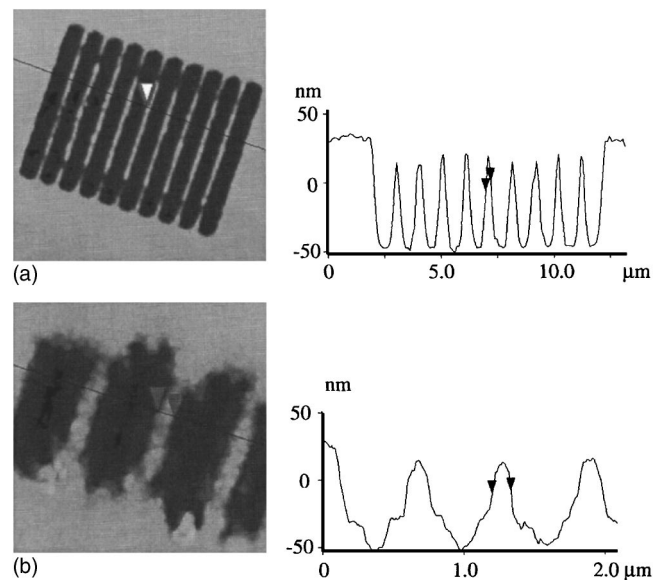


FIG. 3. AFM results of close view and cross section view of the photoresist patterns with (a) 1  $\mu\text{m}$  periodicity and (b) 500 nm periodicity at 90  $\text{W}/\text{m}^2$  using a Ti mask and Ti shield.

phy does not work well with a bare silicon substrate. There is no pattern transfer when the light is weak (the photoresist at the interface is not photoinitiated and washes away during development). On the other hand, when the light intensity is high, the pattern will be significantly oversized. In our approach, a titanium thin film of 80 nm was deposited onto the silicon substrate by electron-beam evaporation. Surface plasmons are also excited on the Ti layer, as shown in the charge density results [Fig. 2(d)]. The charge density distribution appears to be symmetric across the centerline, but with opposite signs. By using this Ti shield, the light intensity is spatially confined to the zone behind the aperture. From the FDTD results we found that, for the gold mask, this zone has a noticeably larger width than the aperture size due to the mismatch of the refractive index of gold (1.74 at 355 nm) with that of air [Fig. 2(b)]. The light transmission through the titanium mask is smaller, but well focused behind the aperture [Fig. 2(c)].

Figure 3 shows Atomic Force Microscopy images of the photoresist line pattern after exposure at an energy density of approximately 90  $\text{W}/\text{m}^2$ . For the gold mask, the line pattern was transferred only with the TM mode to a linewidth of 200–300 nm. For the titanium mask with 1  $\mu\text{m}$  periodicity, both the parallel and perpendicular line patterns, with respect to the laser polarization, were formed with a width of approximately 200 nm [Fig. 3(a)]. The TM mode has a linewidth slightly larger than the TE mode. The 500 nm periodicity pattern is also well defined in the photoresist [Fig. 3(b)] and the TE mode has a linewidth of about 130 nm. By better controlling the light intensity, the linewidth can be decreased.

We also varied the lithographic process by changing laser intensities and dosages for the TM mode gold mask (Fig. 4). As the intensity and dosage increase, the cross section of the lines perpendicular to the laser polarization significantly changed. At a laser energy of about 120  $\text{W}/\text{m}^2$ , the photoresist lines became 300–400 nm in width and two peaks formed across the section [Fig. 4(b)]. The distance between the two peaks is about 200 nm. At this energy level, there was still no pattern transfer parallel to the laser polarization.

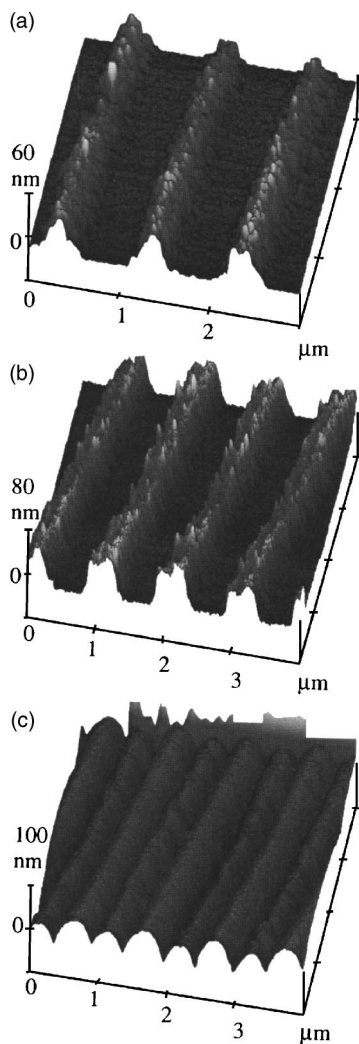


FIG. 4. AFM pictures of photoresist patterns at different energy density and dosage with gold mask and Ti shield. Photoresist lines perpendicular to polarization with (a) 50 s at  $90 \text{ W/m}^2$ , (b) 1 min at  $120 \text{ W/m}^2$ , and (c) 3 min at  $200 \text{ W/m}^2$ .

When the energy density was further increased to about  $200 \text{ W/m}^2$ , the surface plasmon interference effect became significant [Fig. 4(c)]. Additional lines formed between lines of larger height and width. At this energy level, the lines started to form for TE mode but were poorly defined having a noticeable interference effect.

Other mask/shield material combinations were also tested numerically. It has been shown from the FDTD results that the shield material is more crucial than the mask material in this application. Perhaps due to their relatively low refractive index (1.30 for Ti and 1.33 for Cr at 355 nm), titanium and chromium are the best, in terms of confining light intensity, among the many metals commonly used. However, no sufficient light confinement was achieved when

we changed the shield material to an artificial dielectric material (e.g., refractive index 1.3) in the model, indicating the important contribution from free electron plasma. Simulations also revealed that the localization of light does not rely on the periodicity of the pattern on the mask, therefore it is possible to transfer arbitrary patterns for nanolithography.

The 80 nm thick titanium shield was thick enough to absorb the light as it reached the silicon substrate (the penetration depth of titanium at 355 nm wavelength is about 30 nm). Thus, the optical properties of the substrate are not important to the lithography results and virtually any substrate can be used. Once the patterns form in the photoresist, the titanium layer can be used as a metal mask to pattern the substrate. We believe that one may simply replace the laser with a UV lamp in this surface-plasmon-assisted nanoscale photolithography method. The UV light emitted from a mercury lamp peaks at 365 nm, very close to the laser wavelength we used, and the optical properties of gold and titanium do not vary significantly across the peak UV emission wavelength range. With the right mask and additional optics, such as a polarizer, a filter, and an attenuator, we believe that our surface-plasmon-assisted nanolithography technique will extend current photolithography down to a  $\sim 50 \text{ nm}$  scale using existing lithographic equipment.

The authors would like to thank Dr. Heinz Schmid, Dr. Stephen Gray, Dr. Shalom Wind, and Dr. Saiful Khondaker for their helpful input. This work was partially supported by research grants from the US National Science Foundation (Grant Nos. DMI 0222014 and CTS 0243160). Materials characterizations were conducted at the Texas Materials Institute and the Center for Nano and Molecular Science and Technology at The University of Texas at Austin.

<sup>1</sup>S. Okazaki, *J. Vac. Sci. Technol. B* **9**, 2829 (1991).

<sup>2</sup>H. Schmid, H. Biebuyck, B. Michel, and O. J. F. Martin, *Appl. Phys. Lett.* **72**, 2379 (1998).

<sup>3</sup>R. Kunz, M. Rothschild, and M. S. Yeung, *J. Vac. Sci. Technol. B* **21**, 78 (2003).

<sup>4</sup>J. G. Goodberlet and H. Kavak, *Appl. Phys. Lett.* **81**, 1315 (2002).

<sup>5</sup>T. W. Ebbesen, H. J. Lezec, H. F. Ghaemi, T. Thio, and P. A. Wolff, *Nature (London)* **391**, 667 (1999).

<sup>6</sup>L. Salomon, F. Grillot, A. V. Zayats, and F. de Fornel, *Phys. Rev. Lett.* **86**, 1110 (2001).

<sup>7</sup>D. E. Grupp, H. J. Lezec, T. W. Ebbesen, K. M. Pellerin, and T. Thio, *Appl. Phys. Lett.* **77**, 1569 (2000).

<sup>8</sup>W. Srituravanich, N. Fang, C. Sun, Q. Luo, and X. Zhang, *Nano Lett.* **4**, 1085 (2004).

<sup>9</sup>X. Luo and T. Ishihara, *Appl. Phys. Lett.* **84**, 4780 (2004).

<sup>10</sup>J. Pendry, *Science* **285**, 1687 (2002).

<sup>11</sup>E. Popov, M. Nevière, S. Enoch, and R. Reinisch, *Phys. Rev. B* **62**, 16100 (2000).

<sup>12</sup>E. D. Palik, *Handbook of Optical Constants of Solids* (Academic, Orlando, FL, 1985).

<sup>13</sup>S. K. Gray and T. Kupka, *Phys. Rev. B* **68**, 045415 (2003).

<sup>14</sup>P. W. Barber and S. C. Hill, *Light Scattering by Particles: Computational Methods* (World Scientific, Singapore, 1990).